

Computation of Turbulent Premixed Flames response to Inlet Velocity Oscillation

S. Ruan, T.D. Dunstan, N. Swaminathan
University of Cambridge
Cambridge, UK

R. Balachandran
University College London
London, UK

1 Introduction

Combustion instability generally refers to a process where the pressure or velocity fluctuations couple with the unsteady heat release rate in a positive manner leading to growth of the pressure fluctuation which can end up damaging the combustion system. The relation between the velocity perturbation and the heat release rate is typically described by a “Flame Transfer Function” (FTF) $H(A, f)$, with forcing amplitude A and frequency f . It is defined as

$$H(A, f) = Q'_f/u'_f, \quad (1)$$

where Q' and u' is the fluctuation of heat release rate and velocity, normalised by their respective mean value, i.e. $Q' = (Q - \langle Q \rangle) / \langle Q \rangle$. The subscript f denotes a Fourier transform narrow-band filtered around frequency f . The FTF has been studied using theoretical analyses [1], experiments [2] and numerical simulations [3]. Turbulent combustion CFD can provide detailed flow and flame information and thus an ideal candidate to further our understanding of combustion instability issues during the combustor design cycle, or offer insights to determine safe operation envelop and develop control strategies. These instabilities have been modelled using various combustion modelling strategies, such as the Bray-Moss-Libby model [3] and G-equation [1].

Scalar dissipation rate based modelling approach [4] is an alternative flamelet-type combustion model. The importance of the dissipation rate for a reactive scalar and its close relation to the mean reaction rate has been established by Bray [5]. Yet, its accurate modelling remains as a big challenge due to the close coupling among turbulence, mixing and reaction. Recently, there is a significant progress in this topic in turbulent premixed combustion [4]. While the capability of scalar dissipation rate modelling approach has been demonstrated in turbulent premixed flames of different combustion regimes [6], stratified [7] and partially premixed lifted flames [8] and spherical flames [9], its capability in modelling combustion instability has yet to be examined. This study aims to address this gap. Specifically, we like to investigate the model performance in capturing the nonlinear response of turbulent premixed flames under inlet velocity oscillation of different amplitudes and frequencies.

2 Combustion Modelling

The transport equations for the progress variable mean \tilde{c} and variance \tilde{c}''^2 were solved along with other governing equations. The scalar dissipation rate (SDR), $\tilde{\epsilon}_{cc}$, appearing in \tilde{c}''^2 equation, requires modelling. It is defined as $\tilde{\epsilon}_{cc} = \overline{\rho D \nabla c'' \cdot \nabla c''} / \bar{\rho}$, where c'' is the Favre fluctuation. Here, it is modelled as [10]

$$\bar{\rho} \tilde{\epsilon}_{cc} \simeq \frac{\bar{\rho}}{\beta'} \left([2K_c^* - \tau C_4] \frac{S_L^0}{\delta_L^0} + C_3 \frac{\tilde{c}}{k} \right) \tilde{c}''^2. \quad (2)$$

where K_c^*, β', C_3 and C_4 are model parameters detailed in [10]. The unstrained premixed flamelet with presumed PDF model was used to close the mean reaction rate $\bar{\omega}_c = \int_0^1 \dot{\omega}_c(c) P(c) dc$, where $\dot{\omega}_c$ is from the unstrained laminar flame calculation and $P(c)$ is the probability density function obtained using the β function. Combustion kinetics is modelled using a detailed mechanism for ethylene.

3 Experimental Test Case

The experiment by Balachandran *et al.* [2] investigated the nonlinear flame response to velocity forcing. A schematic of the burner setup is illustrated in Fig. 1, which consists of a long tube and a conical bluff body. Gaseous ethylene was injected far upstream and a perfectly premixed mixture was achieved. Inlet velocity oscillation was introduced by loud speakers. The frequency f and the amplitude A of the forcing signals were changed independently over a large range. Measurements of OH^* and CH^* chemiluminescence is performed for the entire flame. Simultaneous CH_2O and OH planar laser-induced fluorescence (PLIF) images for a smaller domain Q^* , indicated in Fig.2(b), were made, from which the Flame Surface Density (FSD) and local heat release rate were then estimated. In this experiment, high amplitude forcing has been applied and non-linear flame response has been observed. It offers a good challenge for modelling as it involves a complex interaction between the turbulent flow and the flames dynamics. The nonlinear response also involves a complex flame behaviour such as roll-up of the flames etc. This experiment has been simulated in [3] using a modified BML and flame surface density model.

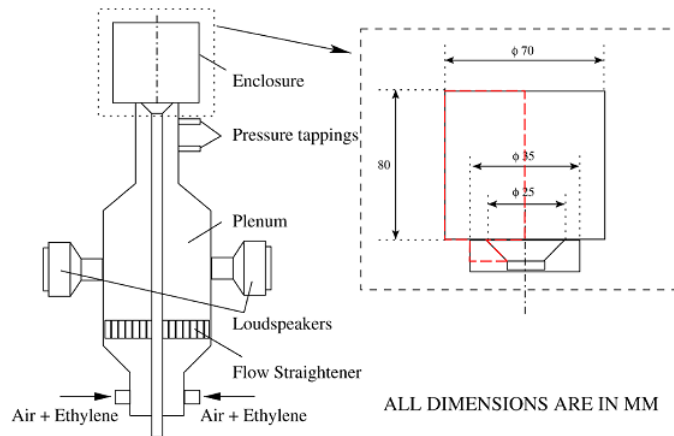


Figure 1: Schematics of the experimental set up in [2]

4 Numerical Setup

The SDR based model has been implemented in a commercial CFD code FLUENT. User defined functions (UDFs) were used to include extra transport equations for \tilde{c} and \tilde{c}''^2 . 2-D axisymmetric unstruc-

tured grid, illustrated in Fig. 2(a) was used. A coarser grid was used for 40Hz case while an adaptively refined grid based on velocity gradient were used for 160Hz case. A pressured based solver with 2nd order discretisation and the SIMPLE pressure-velocity coupling was used. Reynolds stress modelling were chosen to calculated the flow field in order to get a reasonable description of the recirculation zone downstream of the bluff body. The inlet velocity was specified as $U(t) = \langle U \rangle (1 + A \sin(2\pi ft))$ with $\langle U \rangle = 9.9$ m/s.

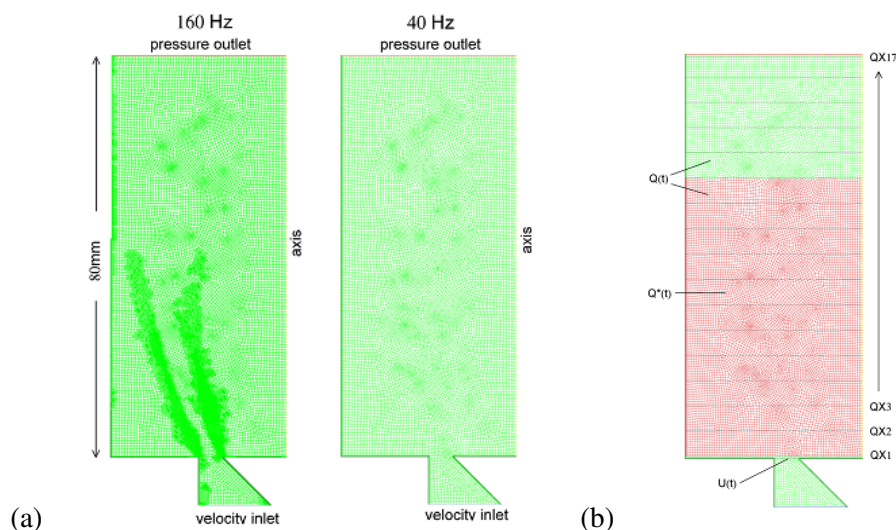


Figure 2: (a) Grid for 160Hz and 40Hz cases. (b) Domain illustration for flame transfer function calculation. Red part corresponds to the size of PLIF measurement.

5 Results and Discussion

For this study, the flame dynamics in response to two frequencies, $f = 40\text{Hz}$ and $f = 160\text{Hz}$ with a range of forcing amplitudes were studied.

Figure 3 presents the comparison of mean reaction rate from the URANS simulation and experimental results of phased averaged flame surface density (FSD) from OH-PLIF for the case of $f = 160\text{Hz}$ and $A = 0.64$ for a phase angle interval of 40 degree, through a complete forcing cycle. At 0° , double flames were observed along the inner and outer shear layers. At 40° , flame in the inner shear layer deforms and subsequently rolls up at 80° . The outer flame also started to deformed and the two flames collapse downstream leading to flame annihilation event. The flames are wrapped around by the vortices and the ‘‘mushroom’’ feature of the two flames at 160° were reproduced. They grew in size and were convected downstream at 200° , subsequently collapsed on the walls at 280° and convected away from the observation domain at 320° . The whole cycle would start again with a new vortex formed at the flame base. In general, the flame dynamics in various phases have been well reproduced by the simulation. A direct comparison highlights the following difference. Two strong flame is observed close to the inlet and the mean reaction rate is substantial along the wall in the simulation, while one strong and a weak flame near the inlet and weak mean reaction rate along the wall are observed in the experiment. The weak reaction in those region might be due to heat loss. Since no quantitative measurement is available, adiabatic wall condition is used in the simulation and resulting in stronger reaction. Investigations including the heat loss effect are required to address this.

In order to evaluate the FTF, the mean and fluctuating heat release rate are required. The mean heat release can either be calculated from the entire computational volume $Q(t)$, as illustrated in Fig. 2(b),

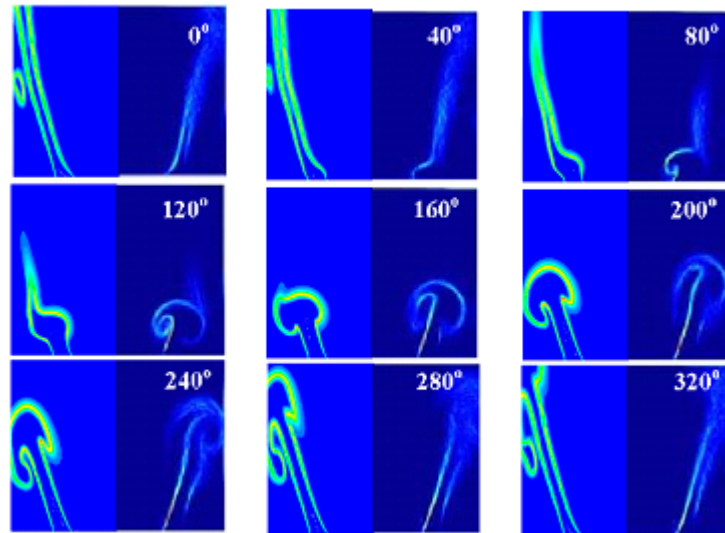


Figure 3: Comparison of mean reaction rate from URANS (left) and FSD from experiment (right) [2] for $f = 160\text{Hz}$ and $A = 0.64$ at different phase angle.

denoted as $\langle Q \rangle$ here; or from the observation window corresponding to the PLIF experiment $Q^*(t)$, as illustrated in Fig. 2(b) also, denoted as $\langle Q^* \rangle$ here. This results in two sets of fluctuating heat release.

Figure 4(a) and (b) present the flame response amplitude obtained from the CFD and experimental results for 40Hz and 160 Hz respectively. Both experimental results obtained from CH^* and OH^* are included. The CFD results obtained from different domains, $Q(t)$ and $Q^*(t)$, were also included. An approximately linear response is evidenced in the case of 40Hz while nonlinear response is clearly evident for 160Hz. In both cases, results obtained from the entire domain $Q(t)$ agree much better with experiment, compared with the results from the truncated domain $Q^*(t)$, which only reproduce the correct trend. This illustrates the importance of including complete information in order to obtain an accurate FTF at the system level, which may not be so in PLIF experiments due to limitation in the observation window size. For the 40Hz case, CFD simulation gives reasonable agreement with experimental results. For the 160Hz case, the simulation shows the flame response amplitude seems to saturate earlier, at forcing amplitude of $A \approx 0.4$ instead of $A \approx 0.6$ in the experiment.

Figure 4(c) and (d) compared the FTF magnitude from the CFD and experiments for 40Hz and 160 Hz respectively. Again, the importance of including the entire domain is clearly evident. Results from truncated domain gives large error in the case of low forcing amplitude. Reasonable agreements between CFD and experimental results are observed for both frequencies, with CFD results slightly underpredicting the FTF magnitude in large forcing amplitudes. This is because as the forcing amplitude increases, the flame tip starts to exit the downstream domain boundary near the cycle maximum and the heat release fluctuation is not fully captured. This issue should be resolved by extending the domain to include the complete flame. Figure 4(e) and (f) present the FTF phase. The CFD generally gives reasonable result but tends to slightly underpredict the phase for low forcing amplitude. To further understand the local flame response, the FTF and heat release rate Q are calculated along line integrals (corresponding to the QXn in Fig. 2b). Figure 5 present the spatial variation of the local flame response under different forcing amplitudes for 40Hz. It can be seen that, heat release rate fluctuations occur only at a certain downstream location for low amplitudes. As A increases, the fluctuations start to occur at upstream locations with higher peak response amplitude. Starting at $A \approx 0.4$, similar heat release response occurs downstream of axial distance of 30mm. Increasing the amplitude results in no obvious difference in the

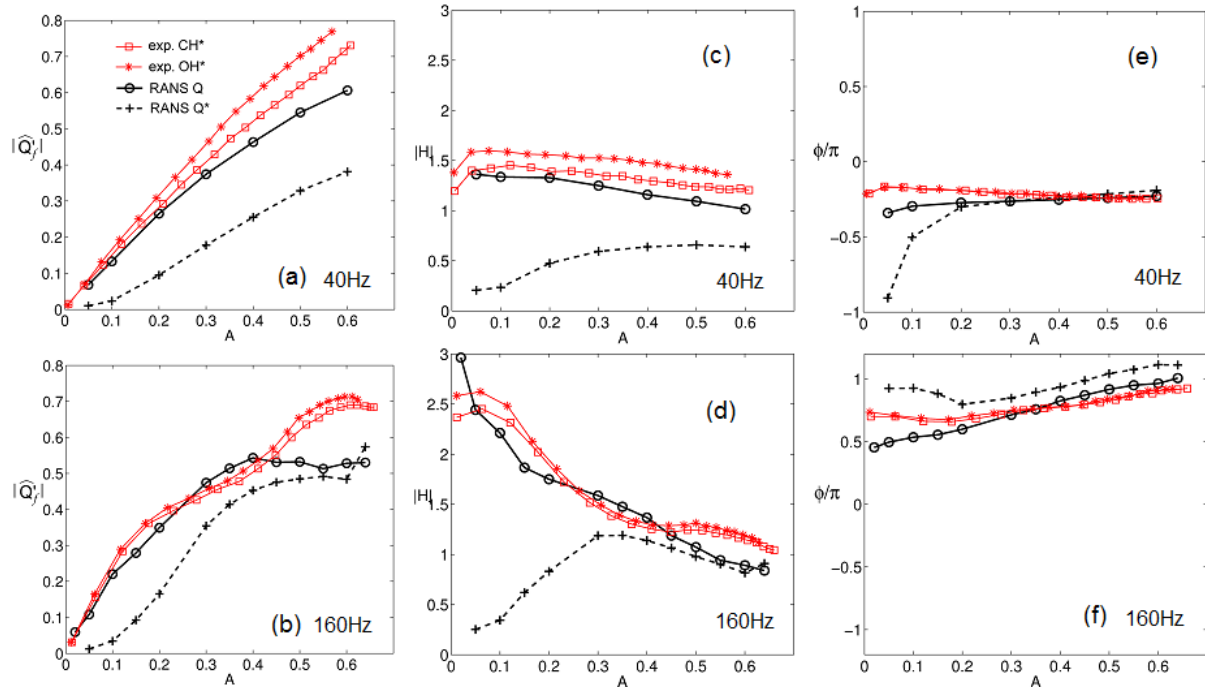


Figure 4: Volumed integrated Flame Transfer Function: (a),(b) Flame response amplitude. (c),(d) Flame Transfer Function magnitude. (e),(f) Flame Transfer Function phases for 40Hz and 160Hz respectively.

flame response downstream of this position. The differences in response are the gradual increase of heat release rate fluctuation at upstream positions. It should be noted that large Q values occur in regions where the flame tip traverses during each cycle. In effect, the high fluctuation is a result of the flame signal becoming bimodal at that particular location. As the amplitude increases, the flame tip reaches further upstream during (or just after) the cycle minimum. We should have seen the same trend for locations further downstream but for amplitudes greater than about 0.2, the flame tip starts to move out from the domain as noted earlier and so it appears to saturate.

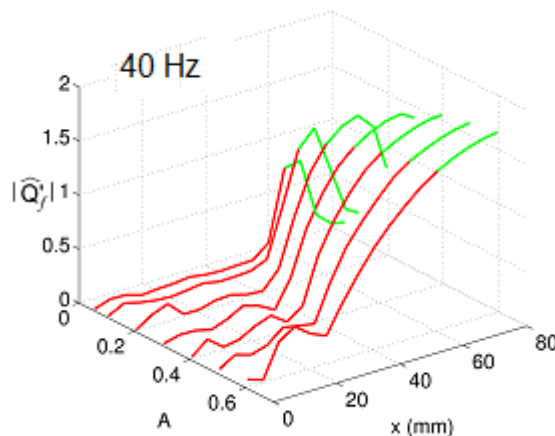


Figure 5: Surface integrated Flame Transfer Function: Spatial variation of flame response amplitude for 40Hz. Red is for domain Q^* and green is for domain $Q - Q^*$ marked in Fig.2.

6 Summary

In this study, the response of turbulent premixed flames stabilised behind a bluff body subject to inlet velocity oscillation was investigated using unsteady RANS simulation. The unstrained laminar flamelet model with presumed PDF method was used to calculate the mean reaction. The scalar dissipation rate model developed in [10] were used in this study. The previous modelling study [3] uses modified BML and an algebraic model for the FSD and thus one step chemistry. The burning mode pdf in the BML model is close to zero and thus it works well for the corrugated flamelets regime. In the current approach, no such restriction applies and detailed chemistry is included using tabulated chemistry. Under different forcing amplitudes and frequencies, both linear and nonlinear flame responses have been observed and agree reasonably well with the experiment. For a fixed amplitude and frequency, the onset of the shear layers roll-up, the gradual development of the flame and vortices as a mushroom type features, and subsequently the collapse of the vortices on the wall, all these features and the entire flame-flow interaction process have been captured well in the computations. Reasonable agreement for the flame transfer function, amplitude, magnitude and phase between the CFD and experiment are obtained. This demonstrates the robustness of the scalar dissipation rate based modelling approach for the mean reaction rate. Further investigation of the overall and local flame response to a wider range of forcing amplitudes and frequencies of inlet velocity oscillation is ongoing.

7 Acknowledgment

The support of Mitsubishi Heavy Industries (MHI), Takasago, Japan is acknowledged gratefully.

References

- [1] T. Lieuwen, Modeling premixed combustion-acoustic wave interactions: A review, *J. Propul. Power* 19 (2003) 765–781.
- [2] R. Balachandran, B. Ayoola, C. Kaminski, A. Dowling, E. Mastorakos, Experimental investigation of the nonlinear response of turbulent premixed flames to imposed inlet velocity oscillations, *Combust. Flame* 143 (2005) 37–55.
- [3] C. Armitage, R. Balachandran, E. Mastorakos, R. Cant, Investigation of the nonlinear response of turbulent premixed flames to imposed inlet velocity oscillations, *Combust. Flame* 146 (2006) 419–436.
- [4] N. Chakraborty, M. Champion, A. Mura, N. Swaminathan, Scalar-dissipation-rate approach, in: N. Swaminathan, K. N. C. Bray (Eds.), *Turbulent Premixed Flames*, Cambridge University Press, 2011, Ch. 2.3, pp. 74–102.
- [5] K. N. C. Bray, The interaction between turbulence and combustion, *Proc. Combust. Inst.* 17 (1979) 223–233.
- [6] H. Kolla, N. Swaminathan, Strained flamelets for turbulent premixed flames ii: Laboratory flame results, *Combust. Flame* 157 (2010) 1274–1289.
- [7] O. R. Darbyshire, N. Swaminathan, S. Hochgreb, The effects of small-scale mixing models on the prediction of turbulent premixed and stratified combustion, *Combust. Sci. Technol.* 182 (2010) 1141–1170.
- [8] S. Ruan, Turbulent partially premixed combustion: DNS analysis and RANS simulation, Ph.D. thesis, University of Cambridge (2012).
- [9] I. Ahmed, N. Swaminathan, Effects of mean curvature on flame propagation, in: 23rd ICDERS, Irvine, USA, 2011.
- [10] H. Kolla, J. W. Rogerson, N. Chakraborty, N. Swaminathan, Scalar dissipation rate modeling and its validation, *Combust. Sci. Technol.* 181 (2009) 518–535.